

## Defects in hydrogenated amorphous silicon-germanium alloys studied by photomodulation spectroscopy

Lingrong Chen and Jan Tauc

*Division of Engineering and Department of Physics, Brown University, Providence, Rhode Island 01912*

J.-K. Lee and Eric A. Schiff

*Department of Physics, Syracuse University, Syracuse, New York 13244*

(Received 17 September 1990)

The sub-band-gap photomodulation (PM) spectra of a series of amorphous hydrogenated silicon-germanium alloys ( $a\text{-Si}_{1-x}\text{Ge}_x\text{:H}$ ) were measured. For dilute alloys ( $x < 0.1$ ) two PM bands were observed. One band had previously been associated with the  $D$  center in unalloyed  $a\text{-Si:H}$ . The relative strength of this band decreased as the alloy parameter  $x$  increased. We associated the second band with a germanium-related  $D$  center ( $\text{Ge-}D$ ). For  $x > 0.1$  only this second ( $\text{Ge-}D$ ) band was observed. The  $\text{Ge-}D$  band's peak was shifted by 0.4 eV from the band gap for the entire range of alloys. We analyzed this band using the assumption that the  $D^0$  and the  $D^-$  levels of the  $\text{Ge-}D$  are symmetrical about the midgap energy. We estimated that the thermal levels of the  $D^0$  and the  $D^-$  are 0.5 eV above the valence-band edge and 0.5 eV below the conduction-band edge, respectively. The result that the levels shift with alloying so as to "track" the band edges differs with some previous work which assumed constant level positions. The relaxation energy was 0.4 eV for all alloys while the effective correlation energy decreased linearly with  $x$  from 0.7 (for  $x=0.1$ ) to 0.0 eV (for  $x=1$ ). A model for the  $\text{Ge-}D$  which may explain its levels' tracking of the band edges is tentatively proposed.

### I. INTRODUCTION

Hydrogenated amorphous silicon-based binary alloys such as  $a\text{-Si}_{1-x}\text{Ge}_x\text{:H}$  and  $a\text{-Si}_{1-x}\text{C}_x\text{:H}$  are currently a subject of much interest in the development of high-efficiency photovoltaic solar cells and other optoelectronic devices.<sup>1</sup> This is because many of the electronic and optical properties of these materials can, in principle, be tuned to match the external requirements by changing the alloy concentration  $x$ . Alloying Si with Ge produces a material with a reduced band gap which better matches the solar spectrum; however, a byproduct of this alloying process is an undesirable increase of the defect density in the band gap.<sup>2,3</sup> There have been numerous studies on the defect states in the gap of  $a\text{-Si}_{1-x}\text{Ge}_x\text{:H}$  alloys using various techniques such as subgap optical absorption,<sup>4</sup> photoconductivity,<sup>5</sup> photoluminescence,<sup>6,7</sup> photoemission,<sup>8</sup> as well as ESR.<sup>9-11</sup> In  $a\text{-Si:H}$ , two kinds of states are considered: tail states at the band edges and  $D$  states deep in the gap. The  $D$  states have been associated with the "dangling" bonds (threefold-coordinated Si atom); more recently, it has been suggested<sup>12,13</sup> that they may be due to fivefold-coordinated Si ("floating" bonds). In the ESR spectrum<sup>9</sup> of  $a\text{-Si}_{1-x}\text{Ge}_x\text{:H}$ , one can identify the Si-related  $D$  state ( $\text{Si-}D$ ) for small  $x$  ( $< 0.1$ ). However, one also observes the signature of another defect whose strength increases with increasing Ge concentration. We shall call it Ge-related  $D$  center ( $\text{Ge-}D$ ).

The  $D$  center is generally accepted as having three charge states: the neutral  $D^0$  state (ground state in the dark) and charged  $D^+$  and  $D^-$  states. In this paper we

make the conventional assumption that most deep levels are neutral in the dark, and thus that charged defects are produced by illumination. There has recently been renewed interest in the possibility that most defects are charged in the dark;<sup>14-16</sup> this would require a relabeling of the optical transitions we describe, but as noted earlier would not otherwise affect the analysis.<sup>17</sup>

The subject of this paper is the determination of the energies of these states in the Ge-related  $D$  center as a function of the alloy composition from which the correlation and relaxation energies can be calculated. The ground state  $D^0$  is seen in the optical spectra in the dark. Recently, Aljishi, Shu, and Ley<sup>8</sup> measured the total-yield photoemission spectra from which they deduced the energy of  $D^0$  with respect to the top of the valence band. They found that this energy did not change with  $x$  and was equal to about 0.4 eV. These measurements do not support the simplest model for a  $\text{Ge-}D$ , in which the defect level would be stationary even as the conduction- and valence-band edges shift with alloying.

Photomodulation (PM) spectroscopy,<sup>18,19</sup> is a method of choice for determining the energies of all three states of the  $D^-$  center. As reported in this paper, we have applied it to study the  $\text{Ge-}D$  center in  $a\text{-Si}_{1-x}\text{Ge}_x\text{:H}$ . We have confirmed the results of Aljishi, Shu, and Ley<sup>8</sup> on the energy of the  $D^0$  state. We have determined the energy of the  $D^-$  state and shown that the  $D^-$  state tracks the conduction band similarly as  $D^0$  tracks the valence band (and at about the same energy of 0.3 eV). It follows that electron correlation energy in the  $D$  center decreases linearly as a function of  $x$  and the lattice relaxation energy of charged states is approximately constant. A model

for the energy levels of the Ge-D centers will be discussed.

## II. EXPERIMENT

The samples were prepared at Syracuse University in a 13.56-MHz plasma deposition reactor. A detailed description of these specimens and a comparison of their properties with previously published results is given in Ref. 20. The substrate temperature was 250°C and the pressure of silane-germane mixtures was 200 mT. Specimen thicknesses varied between 3 and 5  $\mu\text{m}$  as measured using interference fringes. The atomic germanium concentration  $x$  was determined by electron microprobe analysis. The total spin densities  $N_S$  of the specimens are illustrated as a function of the alloy parameter  $x$  in Fig. 1(b).<sup>11,20</sup> Two series of specimens were prepared under nominally identical conditions for the measurements. The first series is represented by the solid symbols in Fig. 1(b). The second series was prepared several months later and is represented by the open symbols. The spin densities of the second series were higher than those of the first. The optical energy gaps of  $a\text{-Si}_{1-x}\text{Ge}_x\text{:H}$  determined from measuring the absorption coefficient  $\alpha$  and using the  $(\omega\alpha)^{1/2}$  vs  $\omega$  plot are shown in Fig. 1(a). We found

$$E_g = 1.75 - 0.75x \text{ (eV)}. \quad (1)$$

It is noteworthy that this simple expression for  $E_g$  in terms of  $x$  holds despite the variability of  $N_S$  with  $x$ . The

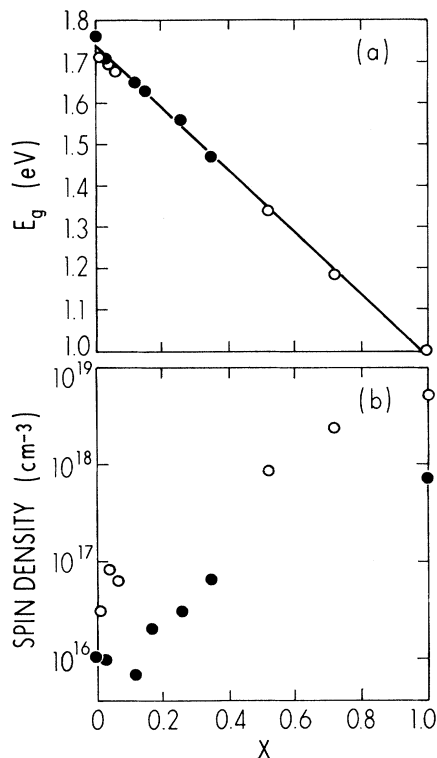


FIG. 1. Characteristics of the samples: (a) optical energy gap  $E_g$  vs composition  $x$ , (b) spin density  $N_S$  vs  $x$  ( $0 \leq x \leq 1$ ).

ESR spectra of the defect system were also determined primarily by  $x$  and were reasonably independent of the spin density.<sup>11,20</sup>

We measured both steady-state and transient PM spectra. For the steady-state PM experiment an  $\text{Ar}^+$  laser beam chopped at 75 Hz was used as the pump beam; its wavelength was 513 nm and its intensity was 50  $\text{mW}/\text{cm}^2$ . The probe beam was an incandescent light source dispersed by a monochromator. The probe energy range was 0.25 to 2.0 eV; the beam was chopped at 500 Hz. By using two asynchronous choppers, the transmittance  $T$  and its photoinduced modulation  $\Delta T$  were simultaneously recorded. For the transient PM experiment, the pump was a Nd:YAG (yttrium aluminum garnet) laser with a dye laser producing pulses of 10-ns width and 2.2 eV photon energy. The probe source was the same as for the steady-state measurements, but instead of the monochromator various band-pass optical filters were used to select spectral ranges.  $\Delta T(t)$  was recorded in the time domain from 100 ns to 50 ms. The details for both experiments have been given elsewhere.<sup>21</sup> The system's spectral response function in both steady-state and transient measurements is canceled by taking the ratio  $-\Delta T/T$ . We assumed that the changes of reflectivity  $\Delta R/R$  are negligibly small compared to  $\Delta T/T$  in these alloys. This assumption was used previously for  $a\text{-Si:H}$ ;<sup>22</sup> in this case the relative changes in transmission  $\Delta T/T$  are equal to the relative changes  $\Delta\alpha/\alpha$  of the absorption coefficient  $\alpha$  if sample thickness  $d > \alpha^{-1}$ .

## III. RESULTS

In this section we report on the photomodulation spectra obtained by steady-state measurements (Secs. III A and III B), and time-resolved measurements (Sec. III C). In Sec. III A we consider samples with small  $x$  so that contributions of both Si- and Ge-related defects can be obtained and compared. At higher concentrations of Ge ( $x > 0.1$ ), the Ge-related defects dominate the spectrum, and in Sec. III B they are studied as a function of composition  $x$ . The time-resolved measurements (Sec. III C) provide additional information for the identification of the defect states.

### A. Steady-state PM spectrum for $x < 0.10$

In Fig. 2 we compare the steady-state PM spectra of  $a\text{-Si:H}$  and  $a\text{-Si}_{0.94}\text{Ge}_{0.06}\text{:H}$ . Figure 2(a) shows the  $a\text{-Si:H}$  PM spectrum measured at 80 K similar to previous work.<sup>19,23</sup> We did not observe detectable changes in the spectrum produced by alloying until  $x \geq 0.03$ . Figures 2(b) and 2(c) show the PM spectra measured at 80 and 150 K on a sample with  $x = 0.06$ . A peak emerged which is apparently associated with Ge alloying. The PM band previously found in  $a\text{-Si:H}$  is more strongly temperature dependent than the Ge-related band. To be more specific, we show in Fig. 3(a) the temperature dependence of PM measured at different probe energies 0.63 and 1.24 eV. The different temperature dependences clearly show that there are two contributions to the spectrum. These results also agree with the ESR measurements of Ref. 20, which show that at  $x = 0.06$ , the Ge-D density becomes

comparable to the Si-D density. Figure 3(b) shows the dependence of the PM signal upon pump intensity at two wavelengths. The slopes of the two curves are almost the same and can be described by a power law  $\Delta\alpha \approx I_\beta$  is about 0.5.

**B. Steady-state PM spectrum for  $x > 0.10$**

The PM spectra for  $x > 0.10$  measured at 300 K are dominated by the Ge-related band (Fig. 4). The spectrum for  $x = 1.0$  (*a*-Ge:H) was measured at 240 K because the signal at 300 K was too small. Only one rather symmetric PM band associated with Ge is observable in the alloys with  $x > 0.1$  at 300 K.<sup>23,24</sup> The band has a gradual onset; the peak shifts with composition  $x$  in the same way as the energy gap  $E_g$ . Similar results have been independently obtained by Chahed *et al.*<sup>25</sup> for  $x \geq 0.36$ .

Figure 5 shows three PM spectra measured at 80, 150, and 300 K for  $x = 0.52$  and Fig. 6 shows three PM spectra measured at 80, 150, and 300 K for  $x = 0.72$ . The PM spectrum does not change much with temperature. The

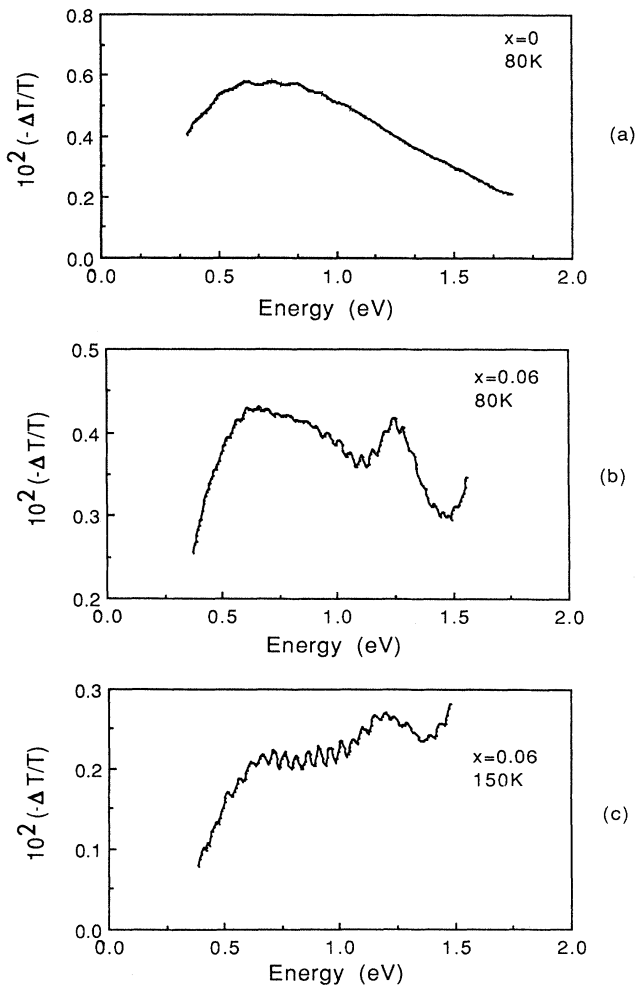


FIG. 2. Steady-state PM spectra (a) *a*-Si:H at 80 K, (b) *a*-Si<sub>0.94</sub>Ge<sub>0.06</sub>:H at 80 K, (c) same specimen as (b) at 150 K.

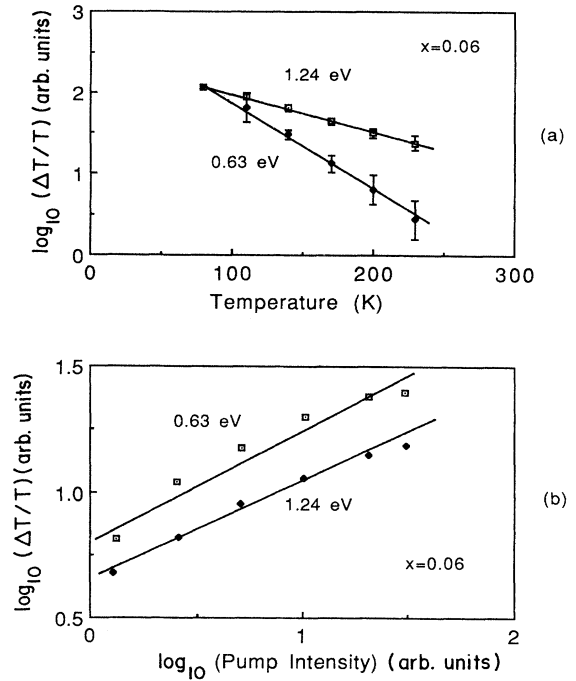


FIG. 3. Temperature (a) and intensity (b) dependences of steady-state PM at 0.63 and 1.24 eV for *a*-Si<sub>0.94</sub>Ge<sub>0.06</sub>:H.

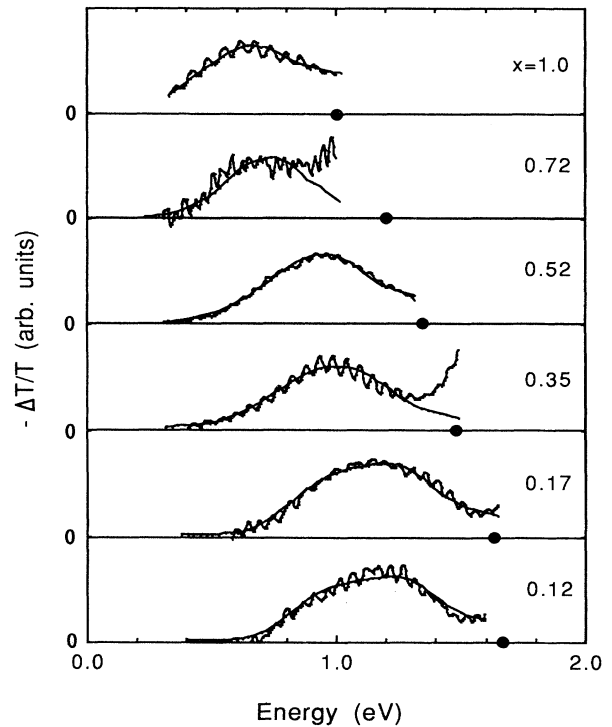


FIG. 4. Steady-state PM spectra at 300 K for compositions with  $x = 0.12$  to 1.0 (spectrum for  $x = 1$  was taken at 240 K). The dots indicate the energy gap  $E_g$ . Solid lines are fits [from L. Chen, J. Tauc, J.-K. Lee, and E. A. Schiff, *J. Non-Cryst. Solids* **114**, 585 (1989). With permission].

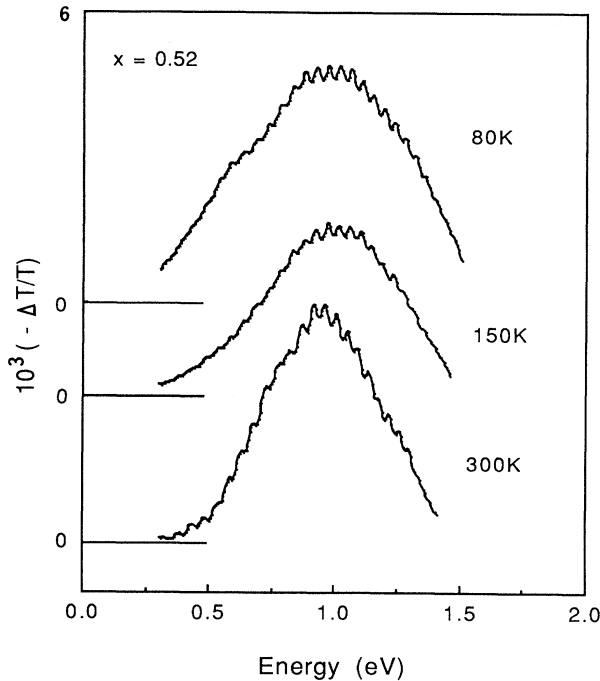


FIG. 5. Steady-state PM spectra for  $a\text{-Si}_{0.48}\text{Ge}_{0.52}\text{:H}$  at 80, 150, and 300 K.

small shifts which were observed are correlated with the temperature dependence of the optical gap. In Fig. 7 we have plotted  $E_g$  as a function of temperature for three alloys. There is little effect of alloying upon  $dE_g/dT$  and this parameter remained close to the value  $4.7 \times 10^4$

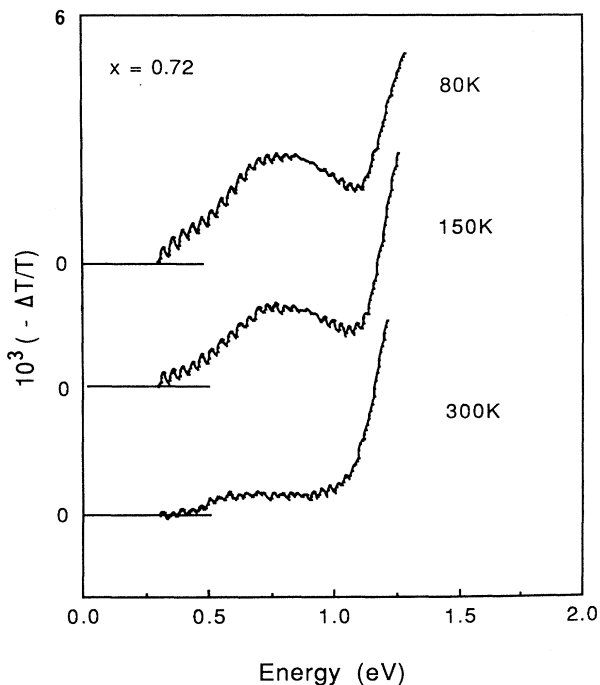


FIG. 6. Steady-state PM spectra for  $a\text{-Si}_{0.28}\text{Ge}_{0.72}\text{:H}$  at 80, 150, and 300 K.

eV/K reported for  $a\text{-Si:H}$ .<sup>26</sup> The onset of photoinduced absorption at the high-energy side of the PM spectra shown in Fig. 6 is due to the thermal effect associated with the temperature dependence of the energy gap.

### C. Transient PM spectrum for $x = 0.35$

In Figs. 8(a)–8(c), we show that the transient PM spectrum of  $a\text{-Si}_{0.65}\text{Ge}_{0.35}\text{:H}$  at three temperatures 80, 150, and 220 K at  $t = 1, 10, 100 \mu\text{s}$ , 1 and 10 ms after the excitation by the laser pulse. We note that the PM spectrum at the longest time (10 ms) is closest to the steady-state PM spectrum while the PM spectrum at the shortest time (1  $\mu\text{s}$ ) is quite different: the low-energy side is much broader and there is a much smaller decrease on the high-energy side. As time increases, the spectrum gradually evolves from the broad spectrum into the rather sharp spectrum observed in the steady-state measurements. The low and high-energy parts of the spectrum change differently with temperature. In the low-energy region, the spectrum decreases with increasing temperature much faster than in the high-energy region. This effect is similar to observations in  $a\text{-Si:H}$ ,<sup>27</sup> in which the low-energy part has been shown to contain contributions of transitions associated with the tail states which decay with time much faster because the carriers in the tail states recombine more quickly than those in the deep states. It is plausible to assume that the same interpretation is applicable to the alloys. There is a difference between  $a\text{-Si:H}$  and  $a\text{-Si}_{1-x}\text{Ge}_x\text{:H}$  alloys: in  $a\text{-Si:H}$ , the contributions of tail states are seen in the steady-state spectrum at low temperature while in the alloys the tail contributions are seen only in the transient spectra at short times.

In the transient spectra of the alloys measured at short times one does not observe a decrease of the PM spectrum at the high-energy side which is observed at long time. This indicates (as explained in more detail later)

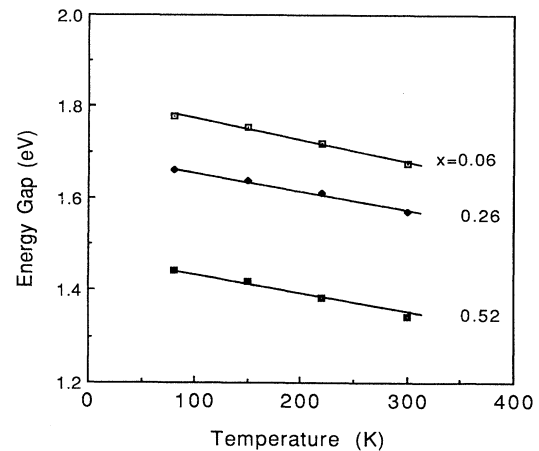


FIG. 7. Temperature dependence of the optical energy gap for  $x=0.06, 0.26,$  and  $0.52$ . The slopes  $dE_g/dT$  are  $-4.40 \times 10^{-4}$  eV/K for  $x=0.06$ ,  $-4.28 \times 10^{-4}$  eV/K for  $x=0.26$ , and  $-4.14 \times 10^{-4}$  eV/K for  $x=0.52$ .

that the trapping of the carriers on a defect which produces the PM spectrum takes a longer time than trapping in a tail state.

#### IV. ANALYSIS

The model used for analyzing the spectra is based on the work of Vardeny and Tauc<sup>28</sup> and Stoddart, Vardeny,

and Tauc<sup>27</sup> on *a*-Si:H. This model assumes that the photoinduced spectra are a superposition of (i) transitions involving the band-tail states and (ii) transitions involving the defects.

In *a*-Si:H, it appears well established that at low temperatures there is a significant contribution of transitions of photogenerated holes trapped in the valence-band tail into the valence band; this contribution is seen in both

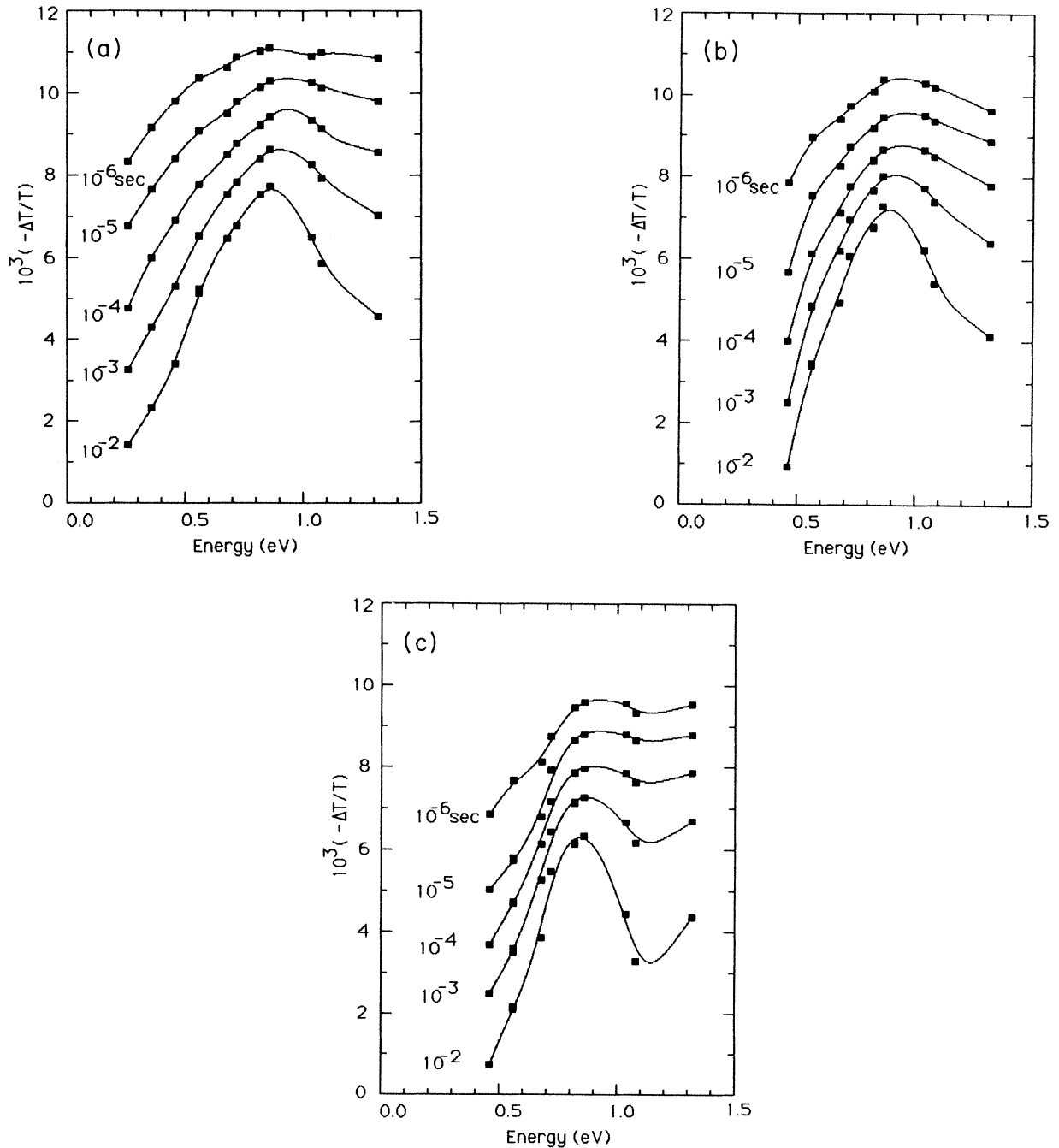


FIG. 8. Transient PM spectra of *a*-Si<sub>0.65</sub>Ge<sub>0.35</sub>:H measured with the probe delays from  $10^{-6}$  to  $10^{-2}$  sec at (a) 80 K, (b) 150 K, (c) 220 K.

the steady-state spectra and time-resolved spectra at low temperature. At low  $T$ , transitions associated with the tail states dominate the spectrum producing a band which is shifted towards low energy with respect to the PM band associated with the defects. A characteristic property of the band-tail contribution is its strong temperature dependence. It decreases much faster with increasing temperature than the defect contribution. This is explained by a shorter lifetime of carriers in the band tail than in the defects at high temperature due to the increased rate of deep hole trapping. In  $a$ -Si<sub>1-x</sub>Ge<sub>x</sub>:H alloys, the contribution of band-tail states is not seen in the steady state at any temperature. Only at low temperatures and very short times do we see transitions with similar characteristics as the tail transitions in  $a$ -Si:H, which is a broadening of the low-energy region of the band that we ascribe to defects [Fig. 8(a), the curve at  $10^{-6}$  sec]. The difficulty of observing the band-tail contribution in alloys relative to  $a$ -Si:H is consistent with the increased rate of deep trapping in the more defective alloys. Since the aim of this paper is to study the properties of the defects, the absence of band-tail carrier PM contribution at room temperature is a useful simplification.

The model for the PM spectra associated with the defect transitions is shown in Fig. 9(a) (this figure does not represent thermal transitions). The defect has ground state  $D^0$ , negatively charged state  $D^-$ , and positively charged state  $D^+$ . The charged states are unrelaxed ( $D^-, D^+$ ) during a time shorter than the relaxation time of the lattice around the defects; at longer times they are relaxed ( $D_r^-, D_r^+$ ). The energy of the unrelaxed  $D^-$  state differs from the energy of  $D^0$  by (bare) electron correlation energy  $U = E^- - E^0$ ;  $E^0$  is the energy of  $D^0$  and  $E^-$  and  $E^+$  are the energies of the unrelaxed states  $D^-$  and  $D^+$ . The relaxed states differ from the unrelaxed states by the relaxation energy  $\Delta E_r^- = E^- - E_r^-$ ,  $\Delta E_r^+ = E^+ - E_r^+$ . The relaxed-state energy  $E_r^-$  and ground-state energy  $E^0$  differ by the effective correlation energy  $U_{\text{eff}} = E_r^- - E^0 = U - \Delta E_r^-$ .

At room temperature we see only one PM band in the alloys for  $x > 0.1$ . As for  $a$ -Si:H,<sup>19</sup> we interpret that as evidence that the energies  $E^-$  and  $E^0$ ,  $E_r^-$  and  $E_r^+$  are symmetrically located about the midgap (it follows that  $\Delta E_r^+ = \Delta E_r^- = \Delta E_r$ ). This is a significant simplification, valid within the precision with which we could discern two bands; we estimate it to be about 0.1 eV.

The PM defect spectra are a superposition of transitions which decrease the absorption [photobleaching (PB)] and transitions which increase absorption [photoabsorption (PA)]. The initial states of PA are always associated with relaxed states; the initial states of PB are always associated with unrelaxed states. The photogenerated electrons and holes are captured at  $D^0$  states transforming them into  $D^-$  and  $D^+$  states. The optical transitions that occur in the dark from the valence band (VB) into the defect state and from the defect state into the conduction band (CB) are bleached. If  $E = 0$  at the top of the VB, then the photon energy for the onset of PB transitions is  $E^-$  because the final state is the unrelaxed  $D^-$  state. Electrons captured in the negatively charged

defects can make transitions into the CB; holes captured in the positively charged defects can make transitions into the VB. These transitions produce PA. However, the PA transitions occur a long time after the carriers are captured and therefore involve the relaxed states  $D_r^-$  and  $D_r^+$ . The photon energy of the PA onset is  $E_g - E_r^- (= E_r^+)$ . It is apparent that if we measure the onsets of PA and PB (and know  $E_g$ ), we can determine all energies in the symmetrical diagram in Fig. 9.

We interpret the simple bands for various compositions (cf. Fig. 4) as an onset of PA which increases with  $\omega$  up to a certain point at which PB sets in and decreases the absorption. One can obtain an approximate value for  $E_g - E_r^- (= E_r^+)$  from an estimate of the onset of the PA band; the maximum of the band approximately corresponds to the onset of the PB transition giving the value of  $E^-$ . More accurate values of these energies can be ob-

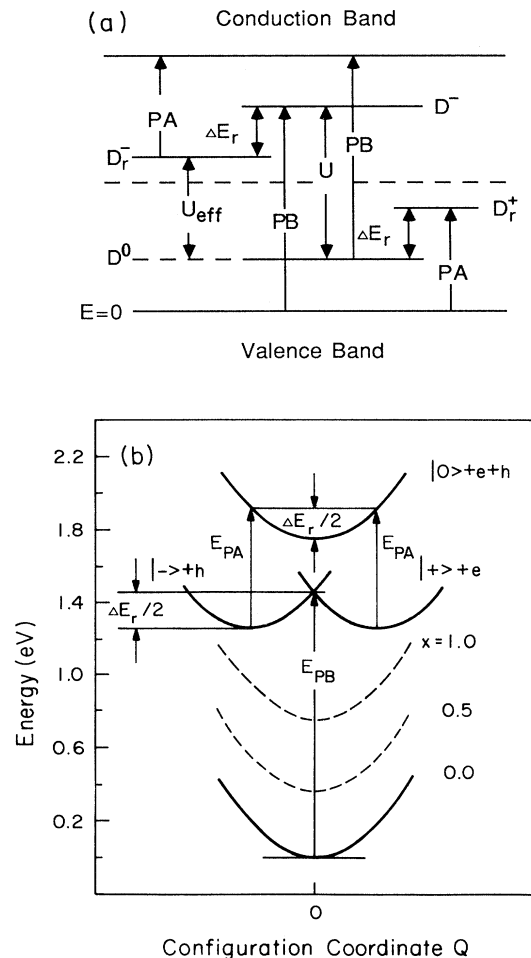


FIG. 9. Energy-level diagrams of the Ge-D center. (a) Combined level diagram and optical transitions. Symmetry about the midgap is assumed. (b) Configurational coordinate diagram. It is assumed that the ground state and charged defect states have the same curvature.

tained by fitting the spectra to a model.

We fitted the spectra of Fig. 4 to a detailed model for the optical transition which includes a distribution of Ge- $D$  level energies. The method has been described previously.<sup>19,21,27</sup> In brief, the defect-states distributions are assumed to be Gaussian  $\exp[-(E-E_d)^2/(\Delta E_d)^2]$  about the respective energies; the widths  $\Delta E_d$  are assumed to be the same for both  $D^-$  and  $D^+$  states. The density of states above the CB and below the VB are assumed to be proportional to the square root of energy and the matrix elements are assumed to be energy independent. The change of the absorption coefficient is calculated as proportional to the convolution of the state densities for both the PA and PB contributions; the total change is obtained by superimposing PA and PB with opposite signs. The expression, beside an arbitrary proportionality constant, has three adjustable parameters for each composition: energies of the peaks of the Gaussian functions for  $D^-$  and  $D^+$  states and their width. These parameters are determined from nonlinear least-square fitting of the data. The accuracy of the energy determination is estimated to be about  $\pm 0.05$  eV.

The fits are drawn as solid lines in Fig. 4. The energy parameters  $E_{PA}$ ,  $E_{PB}$ , and width  $\Delta E_d$  of the fits are shown in Fig. 10 as a function of the alloy composition parameter  $x$ . Referring to Fig. 9(a), we see that the difference  $E_g - E_{PB}$  is identified with the difference in optical threshold energies for two transitions: (i) of an electron from the top of the valence band to the bottom of the conduction band, and (ii) of an electron from the  $D^0$  to the bottom of the conduction band. Using Eq. (1) and the data from Fig. 10 we find that the difference  $E_g - E_{PB}$

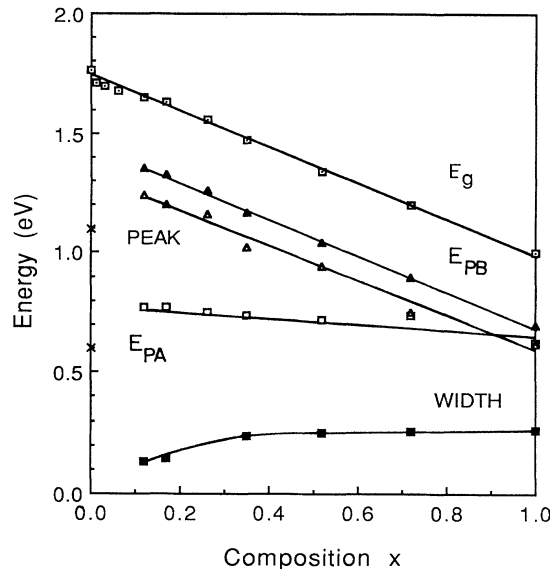


FIG. 10 Dependences of the optical energy gap and the optical transition energies of the Ge- $D$  on alloy composition; the width of the Gaussian distributions is also shown. The crosses on the vertical axis at  $x=0$  show the PA and PB energies of the Si- $D$  in  $a$ -Si:H. [From L. Chen, J. Tauc, J.-K. Lee, and E. A. Schiff, *J. Non-Cryst. Solids* **114**, 585 (1989). With permission.]

is equal to 0.3 eV. The energy difference of optical transitions from these levels to the vacuum estimated without fitting from total-yield photoemission spectroscopy was found<sup>8</sup> to be 0.4 eV. The energy  $E_{PA}$  is 0.7 eV.

As is well known, optical transition thresholds can be significantly larger than thermal transition energies due to relaxation effects. These relaxation energies could not be determined in the photoemission experiment. We estimated  $\Delta E_r$  using the result [see Fig. 9(a)]

$$\Delta E_r = E_{PA} + E_{PB} - E_g, \quad (2)$$

from which we obtained the value  $\Delta E_R \simeq 0.4$  eV independent of alloy parameter  $x$ . The remarkably simple dependence of these fitting parameters upon alloy parameter  $x$  can be compactly summarized in configuration coordinate form, which we have done in Fig. 9(b). The neutral ground state  $|0\rangle$  of the Ge- $D$  is shown for three alloy compositions. For simplicity, the charged states  $|+\rangle$  and  $|-\rangle$  are symmetrically displaced from  $Q=0$ . Each of the curves corresponds to an excitation of the neutral ground state of the defect. For example, the curve labeled  $|+\rangle + e$  at the right is the sum of the energy of the positively charged defect  $D^+$  and an electron at the conduction-band edge; the curve labeled  $|0\rangle + e + h$  is the energy of the neutral defect plus the creation energy of a free electron and hole, which is the band gap  $E_g$ . The increase of Ge concentration shifts the curve  $|0\rangle$  upward toward the curve  $|0\rangle + e + h$  while the three curves do not change; this representation implicitly assumes that alloying does not modify structural relaxation of the Ge- $D$ .

We can obtain the approximate thermal binding energies for the  $D^0$  and  $D^-$  levels using the following expressions for the binding energy of an electron to  $D^-$  and the binding energy of an electron to  $D^0$ , respectively:

$$\Delta E_b^- \simeq \frac{1}{2}(E_{PA} + E_g - E_{PB}) = 0.5 \text{ eV}, \quad (3)$$

$$\Delta E_b^0 \simeq \frac{1}{2}(E_{PB} + E_g - E_{PA}) = E_g - 0.5 \text{ eV}. \quad (4)$$

It is noted that the expressions are exact if the relaxation energies of the transitions  $D^0 + h\nu \rightarrow D^+ + e^-$  and  $D^0 + h\nu \rightarrow D^- + h^+$  are the same, as assumed in Fig. 9(b). The corresponding estimate of effective correlation energy  $U_{\text{eff}}$  is

$$\begin{aligned} U_{\text{eff}} &= E_{PB} - E_{PA} = E_g - E_{PA} - (E_g - E_{PB}) \\ &= E_g - 1.0 = 0.75 - 0.75x \text{ (eV)}. \end{aligned} \quad (5)$$

It follows that the unrelaxed  $D^-$  level is about  $0.7 - 0.4 = 0.3$  eV below the edge of the CB for all compositions  $x > 0.1$ . The bare and effective correlation energies change with  $x$  in the same way as  $E_g$ . The resulting energies of the Ge-related  $D^-$  defect as a function of composition measured with respect to the valence-band edge  $E_v$  (arbitrarily assumed to be zero for all compositions) are shown in Fig. 11. The level positions shown again represent optical, not thermal, transitions. Let us note that the assumption of the energy-level symmetry about the midgap justified above greatly simplifies the analysis and makes it possible to obtain the results shown in Fig. 11.

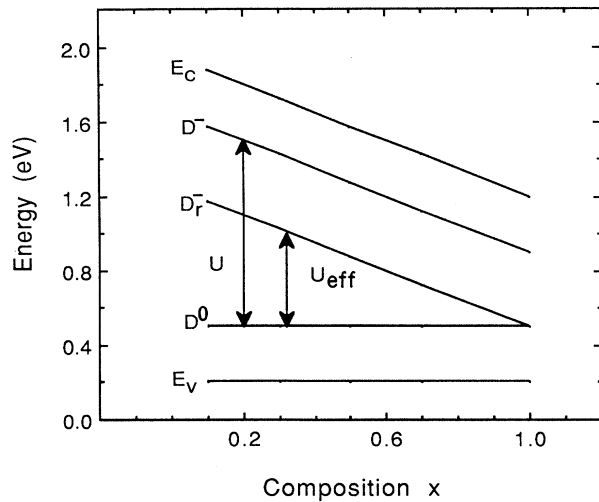


FIG. 11 Dependence of the Ge- $D$  energy levels on composition. The valence-band-edge energy  $E_v$  was arbitrarily selected to be independent of composition.

## V. DISCUSSION

In this research we have shown that the sub-band-gap photomodulation spectrum of  $a$ - $\text{Si}_{1-x}\text{Ge}_x$ :H consists of a single band for alloy parameters  $x > 0.1$ . We attribute this feature to optical transitions involving the Ge- $D$  defect observed in electron-spin resonance. This band is different from the band observed in  $a$ -Si:H, which we attribute to a distinct Si- $D$  defect. For dilute alloys (cf. Fig. 2) the spectrum shows both features, in agreement with the distinction we have drawn.

Remarkably, the peak energy of the Ge- $D$  photomodulation band is shifted from the optical gap of the alloy by 0.4 eV over the entire range of band gaps. This observation is consistent with total yield photoemission measurements (Ref. 8), which revealed a defect feature approximately 0.4 eV above the valence-band edge. An analysis of the PA spectra yielded the energies of the  $D^0$ ,  $D^-$ , and  $D_r^-$  states of Ge- $D$ . The fits show that the  $D^0$  energy [see Fig. 9(a)] is  $0.3 \pm 0.05$  eV above the valence-band edge while  $D^-$  is  $0.3 \pm 0.5$  eV below the conduction-band edge—even as the band edges themselves shift with alloying. We estimate that the thermal levels are 0.5 eV above the valence-band edge and 0.5 eV below the conduction-band edge, respectively.

The existence of two distinct defects can be easily rationalized by identifying the Si- $D$  and Ge- $D$  with well-localized Si and Ge dangling bonds. However, the observation of a constant-energy difference between the Ge- $D$  states and the band edges is not an obvious consequence of this view. For example, the valence-band edge is presumed to be constructed from “weak bonds” between Si and Ge atoms. Photoemission measurements indicate that this band edge shifts 0.4 eV closer to the vacuum as the alloy parameter  $x$  increases from 0 to 1;<sup>8</sup> this shift seems a reasonable consequence of a change in band-tail composition from Si—Si to Ge—Ge bonds. However, it seems unlikely that a simple Ge dangling bond would

shift as much as its backbonds are changed, and indeed in one analysis the energy of the Ge dangling bond has been assumed to be independent of  $x$ .<sup>29</sup>

Both the present photomodulation measurements and also total-yield photoemission measurements indicate that the shift of the Ge- $D$  with increasing alloy parameter  $x$  is the same as the band-edge shift. This observation would be easier to rationalize if the electronic structure of the Ge- $D$  were more similar to the band-tail structure than a simple dangling bond. For this reason we speculate that a singly hydrogenated weak bond is a better identification for the Ge- $D$  than a dangling bond. We leave open the identification of the Si- $D$ . The singly hydrogenated weak bond has been discussed extensively in recent models for defect stability phenomena in  $a$ -Si:H.<sup>30,31</sup>

This proposed identification may also offer an explanation for the surprisingly large effects of alloying on the Ge- $D$  electron-spin-resonance line shape.<sup>11</sup> For low values of  $x$  most Ge- $D$  would arise from Si—Ge bonds, whereas for  $x \sim 1$  most Ge- $D$  centers would originate with Ge—Ge bonds. The ESR line shape for the specimens used in this work is described further in Ref. 20.

We now discuss the results of the detailed analysis of the photomodulation spectrum presented in Sec. IV. First, our curve-fitting procedure indicates that the sum of the absorption and bleaching transition energies of the Ge- $D$  exceeds the band gap of the alloy by a relaxation energy of 0.4 eV. This value is larger than the estimate of 0.1 to 0.2 eV for the Si- $D$ . A difference between the two values would certainly be expected if the two defects had the two different structures we have proposed. However, a quantitative argument along these lines is beyond the scope of this paper and may not be feasible because of the limited reliability of theoretical estimates of relaxation energies at this time.

Lastly we discuss our estimate that the effective electronic correlation energy of the Ge- $D$  declines from 0.7 eV to zero as  $x$  increases from 0.1 to 1; the estimate is based upon the view that the observed photomodulation spectrum consists of two congruent bands belonging to different charge transitions of the Ge- $D$ . Our estimated value of  $U_{\text{eff}}$  is consistent with earlier reports.<sup>29</sup> However, our conclusion that  $U_{\text{eff}}$  for the Ge- $D$  varies substantially with the alloy parameter  $x$  is somewhat unexpected. In some previous work<sup>5,9,29</sup> on defects in the alloys the plausible assumption has been made that the electronic properties of Ge- $D$  are relatively unaffected by the alloy parameter, but this assumption seems inconsistent with the observations reported here. If the present analysis is valid, then the correlation energy of the Ge- $D$  without relaxation is about 0.3 eV less than the band gap over the entire range of alloy composition. This possibility also seems consistent with the proposal that the Ge- $D$  is a hydrogenated weak bond; we presume that this defect electronic structure is a modification of a band-edge state. It seems reasonable to suggest that the band gap may be related to the correlation energy of the band-edge states and thus also to the correlation energy of the singly hydrogenated weak bond structure we have proposed for the Ge- $D$ .



## ACKNOWLEDGMENTS

We thank T. R. Kirst for technical assistance. The work at Brown University was supported by National

Science Foundation Grant No. DMR-870689, at Syracuse University by Solar Energy Research Institute (SERI) Contract No. XB-6-06005-2.

- 
- <sup>1</sup>A. Madan and M. P. Shaw, *Physics and Application of Amorphous Semiconductors* (Academic, San Diego, CA, 1988), Chap. III.
- <sup>2</sup>F. Finger, W. Fuhs, G. Beck, and R. Carius, *J. Non-Cryst. Solids* **97/98**, 1015 (1987).
- <sup>3</sup>R. A. Street, C. C. Tsai, M. Stutzmann, and J. Kakalios, *Philos. Mag.* **B 56**, 289 (1987).
- <sup>4</sup>S. Aljishi, Z. E. Smith, and S. Wagner, *Amorphous Silicon and Related Materials*, edited by H. Fritzsche (World Scientific, Singapore, 1989), p. 887.
- <sup>5</sup>K. D. Mackenzie, J. R. Eggert, D. J. Leopold, Y. M. Li, S. Lin, and W. Paul, *Phys. Rev. B* **31**, 2198 (1985).
- <sup>6</sup>R. Ranganathan, M. Gal, J. M. Viner, and P. C. Taylor, *Phys. Rev. B* **35**, 9222 (1987).
- <sup>7</sup>R. Carius, *Amorphous Silicon and Related Materials*, edited by H. Fritzsche (World Scientific, Singapore, 1989), p. 939.
- <sup>8</sup>S. Aljishi, Jin Shu, and L. Ley, *Amorphous Silicon Technology—1989*, edited by A. Madan *et al.* (Materials Research Society, Pittsburgh, 1989), p. 125.
- <sup>9</sup>M. Stutzmann and R. J. Nemanich, *Phys. Rev. B* **30**, 3595 (1984).
- <sup>10</sup>W. Fuhs and F. Finger, *J. Non-Cryst. Solids* **114**, 387 (1989).
- <sup>11</sup>J.-K. Lee and E. A. Schiff, *J. Non-Cryst. Solids* **114**, 423 (1989).
- <sup>12</sup>S. J. Pantelides, *Phys. Rev. Lett.* **57**, 2979 (1986).
- <sup>13</sup>R. Biswas, C. Z. Wang, C. T. Chan, K. M. Ho, and C. M. Soukoulis, *Phys. Rev. Lett.* **63**, 1491 (1989).
- <sup>14</sup>H. M. Branz, *Phys. Rev. B* **39**, 5107 (1989).
- <sup>15</sup>T. Shimizu, M. Kidoh, M. Matsumoto, A. Morimoto, and M. Kumeda, *J. Non-Cryst. Solids* **114**, 630 (1989).
- <sup>16</sup>J. Ristein, J. Hautula, and P. C. Taylor, *J. Non-Cryst. Solids* **114**, 444 (1989).
- <sup>17</sup>Y. Bar-Yam, J. D. Joannopoulos, and D. Adler, *Phys. Rev. Lett.* **55**, 138 (1985).
- <sup>18</sup>J. Tauc and Z. Vardeny, *Philos. Mag.* **B 52**, 313 (1985).
- <sup>19</sup>Z. Vardeny, T. X. Zhou, H. Stoddart, and J. Tauc, *Solid State Commun.* **65**, 1049 (1988).
- <sup>20</sup>J.-K. Lee and E. A. Schiff (unpublished).
- <sup>21</sup>H. A. Stoddart, Ph.D. thesis, Brown University, 1987.
- <sup>22</sup>H. T. Grahn, C. Thomsen, and J. Tauc, *Opt. Commun.* **58**, 226 (1986).
- <sup>23</sup>P. O'Connor and J. Tauc, *Phys. Rev. Lett.*, **43**, 311 (1979).
- <sup>24</sup>D. Pfof, H. -N. Liu, Z. Vardeny, and J. Tauc, *Phys. Rev. B* **30**, 1083 (1984).
- <sup>25</sup>L. Chahed, A. Gheorghiu, M. L. Theye, I. Ardelean, C. Senemaud, and C. Godet, *J. Non-Cryst. Solids* **114**, 471 (1989).
- <sup>26</sup>G. D. Cody, T. Tiedje, B. Abeles, B. Brooks, and Y. Goldstein, *Phys. Rev. Lett.* **47**, 1480 (1981).
- <sup>27</sup>H. A. Stoddart, Z. Vardeny, and J. Tauc, *Phys. Rev. B* **38**, 1362 (1988).
- <sup>28</sup>Z. Vardeny and J. Tauc, *Phys. Rev. Lett.* **54**, 1844 (1985).
- <sup>29</sup>M. Stutzmann, R. A. Street, C. C. Tsai, J. B. Boga, and S. E. Ready, *J. Appl. Phys.* **66**, 569 (1989).
- <sup>30</sup>K. Winer, *Phys. Rev. B* **41**, 12 150 (1990).
- <sup>31</sup>Sufi Zafar and E. A. Schiff, *Phys. Rev. B* **40**, 5235 (1989).